Can We Compute The Worst Voltage Case Under Power Flows Uncertainty at TSO-DSO Interfaces?

Florin Capitanescu
Environmental Research and Innovation (ERIN), Luxembourg Institute of Science and Technology (LIST)
Belvaux, Luxembourg
florin.capitanescu@list.lu

***Abstract*—This paper proposes the new problem of calculating the worst-voltage-case (WVC) under power flows uncertainty, particularly at interfaces between transmission and distribution grid operators. The goal of the calculation is to verify if the realization of the worst uncertainty scenario leads to abnormal voltages, or assure where the voltage instability is not a risk, and inform the transmission system operator. The problem is formulated as a tailored non-convex, nonlinear optimal power flow (OPF) with complementarity or equilibrium constraints (ECs). The latter model the generator switch between under voltage control and under reactive power limit. The problem is converted into a mathematically equivalent nonlinear programming OPF problem in which ECs are handled as penalty terms in the objective function. The paper has conducted a series of experiments on the 60-bus Nordic system, which have pointed out the challenges associated to such computations to obtain meaningful results and unveiled new insights. The findings and scalability are confirmed using a real-world 1203-bus system.**

***Index Terms*—optimal power flow, TSO-DSO coordination, uncertainty, worst-case computation, voltage stability**

I. Introduction

Transmission systems operators (TSOs) are facing growing uncertainty in operation especially due to:

- large presence of variable renewable energy (VRE) generation, wind and solar power, in the transmission grid;
- the increase, yet little matched, of the generation and consumption in distribution systems, caused by VRE sources (particularly solar and storage), as well as the electrification of other energy sectors, materialized by a fast penetration of electric vehicles and heat pumps;
- increased variability of the power flows through interconnection lines with neighbour systems.

This operation uncertainty also materializes through alarming wider ranges and growing variability of power flows at the interfaces (i.e. physical substations) of the networks managed by transmission and distribution system operators (TSOs and DSOs). This motivates enhancing the coordination between the operations of TSOs and DSOs [1], [2]. However, independently of the mechanisms for TSO-DSO coordination, the uncertainty issue requires special attention by the TSOs. Specifically, it is of interest for a TSO to evaluate whether the worst realization of uncertainty, within some realistic ranges, can harm the transmission network operation reliability in various respects (congestion, voltage, stability, etc.). A particularly interesting and reassuring outcome is if these purposedly-conservative WVCs turn out not to threaten reliable operation.

While there are works focusing on how the DSOs can dispatch the distribution grid assets to support transmission grid voltages [3], [4], [5], their efficiency depends on weather conditions, e.g. sun and wind. However, extreme, yet likely, situations of no or little VRE production and high load in some distribution grids may lead to unacceptably low voltages or even trigger voltage instability in the transmission grid.

This paper focuses on computing worst-case operation scenarios under uncertainty for low or unstable voltages. The goal of such computation is to identify and inform the TSO whether potential voltage issues may appear. The TSO may decide based on different tools how to handle such situation.

This work falls under the framework of AC optimal power flow (OPF) under uncertainty, specifically robust OPF [6]. However, it should be emphasized that, well before this framework, conceptually similar research has been conducted to calculate the minimum distance to the operation feasible region boundary under uncertainty. For instance, calculating the worst operation case of a power system under load uncertainty has been researched in the framework of security margins [7], [8], [9], [10]. These approaches calculate minimum security margins under uncertainty with respect to overloads [8], [10] or voltage instability [7], [9], [10]. These approaches tackle min-max (or robust) optimization problems as a security margin is the maximum value of the (loading) parameter that a system can sustain along a given direction.

The framework of AC OPF under uncertainty responds to the TSOs' need in departing from the provision of optimal solutions of the most likely operation scenario. The presence of uncertainty adds a major complexity and computation burden to conventional decision-making tools of operators, that have to be leveraged from deterministic (i.e. most likely forecast) to uncertainty-aware [6]. The most prominent works rely on robust optimization [11], [12], [13]. Furthermore, some works have leveraged robust optimization techniques to AC security-constrained OPF (SCOPF) [14], [15], [16] relying on the computation of the worst case scenario for a contingency, formulated as a bi-level (min-max) AC OPF problem.

This work is supported by Luxembourg National Research Fund (FNR) in the frame of the project ECHO (INTER-DFG/22/15625441/ECHO).

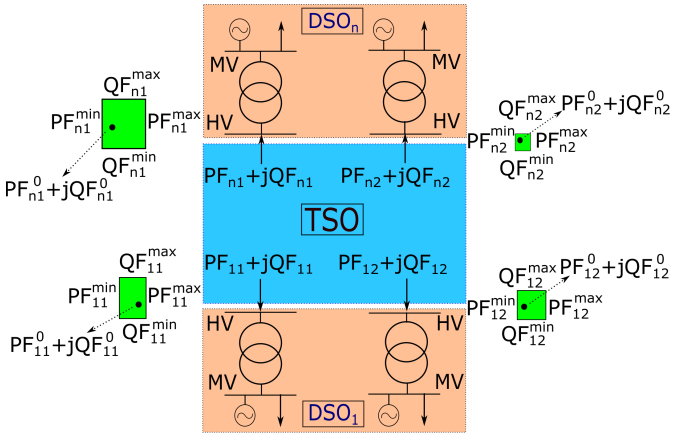

Fig. 1. Box uncertainty sets (colored in green) of real and reactive power flows at four TSO-DSO interfaces.

The worst case calculations (of this work) can inform or be part of robust optimization algorithms for AC OPF or SCOPF.

While the worst-overload-case can be addressed in a simpler and sound way [15], the same methodology cannot be applied for the worst-voltage-case as the worst uncertainty may point in directions where there is no feasible solution of the problem.

The new contribution of the paper is the problem to compute the WVC under power flow uncertainty at TSO-DSO interfaces. The paper reveals the challenges to such computations to obtain meaningful solutions and yields new insights.

II. The Worst Voltage Case (WVC) Problem

The worst-case calculation needs first defining the uncertainty in a given system operating state. Without loss of generality, in this work the uncertainty is modeled as variable, within some bounds, and uncorrelated[1] active and reactive power flows at TSO-DSO interfaces (substations) for distribution grids with high VRE penetration.

The assumed uncertainty box is modelled by the constraints (2)-(3), see the green boxes in Fig. 1 related to four TSO-DSO interfaces. The parameters PF_i^0 and QF_i^0 are the active and reactive powers forecasted at the TSO-DSO interface (bus) i. The optimization variables PU_i and QU_i model the uncertainty of active and reactive power flows (e.g. forecasting errors) at node i. The bounds of the uncertainty boxes, i.e. extreme active/reactive power flows (parameters $PF_{11}^{\min}$, $QF_{11}^{\max}$, etc.), can be positive or negative and be inferred from historical data, if available.

The WVC problem requires pre-selecting the critical interface (node), denoted by k, which will experience the worst (i.e. lowest) voltage magnitude whatever the realization of uncertainty within the set. It is assumed that the TSO experience and knowledge of the system allows selecting the critical node seamlessly. Otherwise, fast sensitivities of node voltage drop to uncertain powers change can be used rank the candidate nodes. Further, solving (in parallel) the WVC problem for each of the top ranked candidate nodes is not a computation bottleneck. Optimizing over a set of candidate nodes may be contemplated to reveal problematic voltage cases but not the worst-case.

The proposed tailored WVC AC OPF formulation is expressed in polar voltage coordinates (V, θ) as follows:

$$\min V_k \tag{1}$$

$$\text{s.t. } PF_i^{\min} \le PF_i^0 + PU_i \le PF_i^{\max}, \qquad \forall i \in \mathcal{N} \tag{2}$$

$$QF_i^{\min} \le QF_i^0 + QU_i \le QF_i^{\max}, \qquad \forall i \in \mathcal{N} \tag{3}$$

$$PG_i - PF_i^0 - PU_i - \sum_{j \in \mathcal{B}_i} P_{ij}(V_i, V_j, \theta_i, \theta_j) = 0, \qquad \forall i \in \mathcal{N} \tag{4}$$

$$QG_i - QF_i^0 - QU_i + b_i V_i^2 - \sum_{j \in \mathcal{B}_i} Q_{ij}(V_i, V_j, \theta_i, \theta_j) = 0, \qquad \forall i \in \mathcal{N} \tag{5}$$

$$PG_i = PG_i^0, \qquad \forall i \in \mathcal{G} \setminus \{s\} \tag{6}$$

$$PG_i^{\min} \le PG_i \le PG_i^{\max}, \qquad i = s \tag{7}$$

$$I_{ij}(V_i, V_j, \theta_i, \theta_j) \le I_{ij}^{\max}, \qquad \forall i, j \in \mathcal{N} \tag{8}$$

$$V_i^{\min} \le V_i \le V_i^{\max}, \qquad \forall i \in \mathcal{N} \setminus \mathcal{G} \tag{9}$$

$$V_i^{\min} \le V_i \le V_i^0, \qquad \forall i \in \mathcal{G} \tag{10}$$

$$QG_i^{\min} \le QG_i \le QG_i^{\max}, \qquad \forall i \in \mathcal{G} \tag{11}$$

$$(QG_i^{\max} - QG_i) \perp (V_i^0 - V_i), \qquad \forall i \in \mathcal{G} \tag{12}$$

where: V_k is the voltage magnitude at the critical node k, PG_i/QG_i are the real/reactive powers generated at node i, $PF_i^0 + PU_i$/$QF_i^0 + QU_i$ are total uncertain real/reactive power flows (seen as loads by the TSO) at any TSO-DSO interface, PG_i^0 is the fix real power production of the generator at node i, b_i is the susceptance of shunt capacitor/reactor at node i, V_i and θ_i are the magnitude and angle of complex voltage at node i, V_i^0 is the voltage setpoint of the generator at node i, P_{ij}/Q_{ij} are the real/reactive power flows on the branch linking nodes i and j, I_{ij} is the current through the branch linking nodes i and j, $X^{\min}$ and $X^{\max}$ are lower and upper bounds on given quantity X, $\mathcal{N}$ is the set of nodes, $\mathcal{G}$ is the set of generators, $s \in \mathcal{G}$ corresponds to the slack generator, $\mathcal{B}_i$ is the set of branches connected to bus i, and the operator $\perp$ denotes the complementarity of two quantities.

The meaning of problem constraints is as follows. Uncertain power flows are limited at each individual node by constraints (2)-(3). Constraints (4)-(5) are the nodal active and reactive power balance, affected by the corresponding uncertainty PU_i and QU_i, respectively. Constraints (6)-(7) express that, for the sake of simplicity, only one slack generator s (using distributed slack would enhance the model realism) compensates the mismatch due to uncertain real power flows and losses. Constraints (8)-(9) express operation limits on branch current and bus voltage magnitude, respectively. Constraints (11) model physical limits of generators' reactive power.

The ECs (12) are essential and express that a generator can be either under voltage control (i.e. $V_i = V_i^0$) or in the maximum reactive power limit (i.e. $QG_i = QG_i^{\max}$), in which case its terminal voltage V_i may drop below its setpoint V_i^0 as

[1]Correlations between the uncertain active and reactive powers at a node can be straightforwardly modelled.

per (10). Since one looks for the lowest voltage, that normally may harm only at high load, ones does not expect (hence not model) a generator reaching its minimum reactive power limit.

The above OPF formulation is a non-convex, nonlinear, robust OPF problem with ECs. The uncertain powers PU_i, QU_i are the driving decision variables; they attempt lowering the voltage at the critical node, especially by forcing some generators to reach the maximum reactive power limit and lose the control of their terminal voltage, which will drop.

Note that, as it will be numerically demonstrated, since one searches the lowest voltage, the choice of $V_i^{\min}$ is critical for obtaining meaningful results.

Nonlinear optimization problems with ECs cannot be solved reliably by off-the-shelf solvers because the Mangasarian-Fromovitz constraint qualification is not met and thereby the feasible regions practically vanishes creating numerical challenges at the point where ECs should be met. Severe convergence issues of AC OPF with ECs were reported [17].

To avoid such numerical issues, the problem is converted into a mathematically equivalent nonlinear program (NLP) AC OPF problem in which ECs (12) are handled as penalty terms in the objective function, leading to the augmented objective:

$$\min\{V_k + \omega \sum_{i \in \mathcal{G}} (QG_i^{\max} - QG_i)(V_i^0 - V_i)\} \qquad (13)$$

The penalty term ensures that a generator' terminal voltage does not drop from its setpoint unless the generator reaches its maximum reactive power limit. The penalty parameter ω should be slightly tuned in practice. However, a rough rule to set it consists in imposing that the penalty term should not affect by more than ε_V the value of the worst voltage. Hence, $\omega \geq \varepsilon_V/(|\mathcal{G}|\varepsilon_F^2)$, where $|\mathcal{G}|$ is the number of generators able to control the voltage and ε_F is the feasibility tolerance of the AC OPF constraints, except the ECs. Typical values may be $\varepsilon_V = \varepsilon_F = 10^{-4}$.

The AC OPF problem (13), (2)-(11) is thus an NLP problem that can be solved by existing solvers. However, while the combinatorial nature of the problem due to the ECs cannot be removed or the global optimum guaranteed, the reformulation guarantees a feasible, at least local optimal solution.

III. Numerical Experiments

A. Experiments Set-Up

The subsequent experiments have been conducted first and mostly on a 60-bus model of the Nordic system, see Fig. 2 [18]. The findings and scalability have been then validated using a real-world 1203-bus system.

The Nordic system has 60 nodes, 23 generators, and 22 TSO-DSO interfaces modeled as net loads. In all experiments only the slack generator g22, see the figure, balances the MW changes and losses caused by the uncertainty.

Upper voltage limit is set to 1.1 p.u. in all experiments. Lower voltage limit is set to a different value in each experiment, specified later. Generators control their initial terminal voltage as long as they do not attain the reactive power limit. After tunning, the penalty ω is set to 1000.

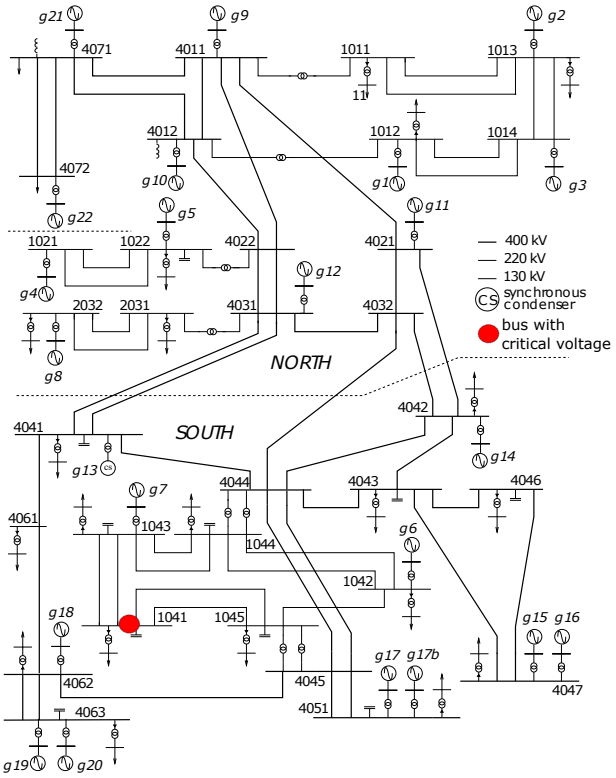

Fig. 2. One-line diagram of the 60-bus system.

The NLP problems have been coded in GAMS (version 28.2) [19] and solved by IPOPT [21] solver on a PC of 2.7-GHz and 8-GB RAM.

The uncertainty is specifically defined as variable and independent active/reactive power flows at any TSO-DSO interface (load bus), limited by a same proportion ρ of the active/reactive load power, see constraints (2)-(3). Specifically, $\forall i \in \mathcal{L}$: $-\rho PF_i^0 \leq PU_i \leq \rho PF_i^0$, and $-\rho QF_i^0 \leq QU_i \leq \rho QF_i^0$.

B. First Set of Experiments: Relaxed Low Voltage Limit

These experiments compute the lowest voltage value at the critical node 1041 (see Fig. 2) for increasing uncertainty ranges, steered via the uncertainty budget ρ (see Table I). IPOPT is initialized by using a flat start for voltages. Low voltage bound is relaxed to $V_i^{\min} = 0.1$ p.u., $\forall i \in \mathcal{N}$.

TABLE I
Experiments and Uncertainty Budget

experiment	ρ (%)	worst voltage (p.u.)
A	20	0.947
B	25	0.889
C	26	0.869
D	26.95	0.833
E	26.995	0.823
F	27	**0.131**

Fig. 3 shows the objective of the optimization problem, i.e. the lowest voltage magnitude obtained at bus 1041, for the six experiments, A to F. One can observe that, as expected, the larger the uncertainty budget the worse the voltage value.

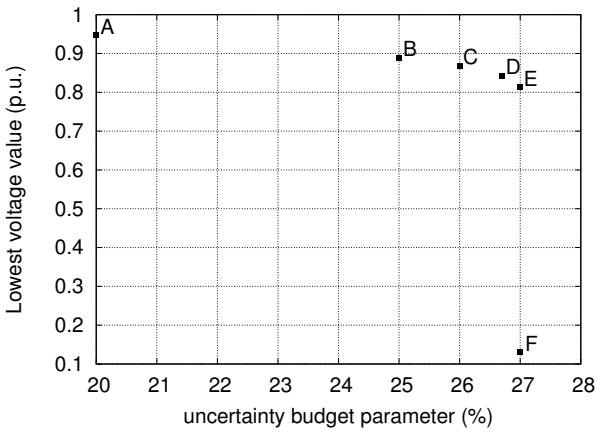

Fig. 3. Worst voltage versus uncertainty budget.

It should be noted that the point E corresponds practically to a loadability limit of the system. Indeed, in a separate calculation, a proportional load increase is applied to the same loads that form the uncertainty set and the so-obtained loadability margin equals 26.9975% of load increase.

The huge difference of voltages between points E and F as well as the extremely low voltage at point F (0.13 p.u.), for a small increase (of 0.005%) in the uncertainty budget, are striking. Indeed, the worst voltage drops sharply between the two points form roughly 0.82 p.u. to 0.13 p.u..

To facilitate results interpretability and reproducibility, Tables II and III provide the voltage at nodes and generators' reactive power. From Table II one can notice that, except point F, voltages at load buses drop progressively as the budget of uncertainty grows. From Table III one can remark that three generators, whose figures are highlighted in bold, have reached the reactive power limit before a loadability limit is attained, namely g5 at point C, g7 at point D and g6 at point E.

One can conclude that the proposed model works well numerically until the uncertainty budget can create infeasible problems, i.e. until a loadability limit (emphasizing that uncertainty can push the system to different loadability limits). Once the budget of uncertainty can push the system beyond a loadability limit, the worst voltage drops extremely low (at 0.131 p.u.) while the uncertainty naturally distributes in such a way to maintain appropriate voltages in the system. More precisely, the uncertainty creates counter-flows to relieve the system stress, except the few nodes around the critical load, see three critical voltages, particularly the voltage at only one generator, g7, drops to 0.69 p.u.. Accordingly, due to a stress relieve, only the generator g7 reaches its reactive power limit as compared to three generators being in a limit for point E.

The main explanation of the difference between points E and F is that, as the uncertainty budget is larger in the case F, the optimization algorithm searches beyond point E and converges to a better local optimum than point E.

Therefore, searching the lowest voltage magnitude at a node and not imposing a realistic lower limit on it in the optimization are conflicting. As the flat initialization of IPOPT is reasonable, the solver converges to lower and lower voltage including after a breaking point (loadability limit).

The results confirm that the ECs are correctly handled as penalty terms in the objective function. Indeed, by looking at these tables one can notice that all generators maintain their voltage setpoint unless they are at the reactive power limit, in which case the voltage drops.

C. Second Set of Experiments: Impact of Low Voltage Limit

This set of experiments consists of two variants of experiment C (C1, C2) and three variants of experiment F (F1, F2, F3); their characteristics are provided in Table IV.

Table IV indicates that the lower the voltage limit, the lower the objective as well as, except case C2, the objective coincides with the low voltage bound.

Tables V and VI show that the lower the voltage limit, further generators reach their reactive power limit, their terminal voltage dropping accordingly. If the uncertainty budget is not significant and the voltage limit is sufficiently low, as in case C2, no voltage limit is attained. In fact, the results for experiment C2 are the same as for C and hence further results are not reported. If the uncertainty is not significant and the voltage limit has a high value, as in case C1, the low voltage limit is reached, preventing computing the true worst-case.

Very interesting, if the uncertainty budget can lead to infeasible problems, as in experiments F1 to F3, the uncertainty is adjusted such that the low voltage limit is always reached, stopping the degradation to the worst voltage (0.131 p.u.) computed in case F for this uncertainty budget. Therefore, for this budget of uncertainty, lowering the voltage limit allows fully exploring the lower part of the power-voltage (PV) curve widely used in voltage stability analysis.

D. Third Set of Experiments: Impact of Voltage Initialization

Using the same assumption as for the experiment B (i.e. $V_i^{\min} = 0.1$ p.u.) one studies the effect on the worst voltage of the voltage magnitude initialization in IPOPT solver, see Table VII. The results indicate that as long as the initial voltages are larger than 0.80 p.u. the solver converges to the same worst voltage solution (0.889 p.u.) as in case B; so cases B and B2 are identical. However, very interestingly, when voltages are initialized with values below 0.75 p.u. IPOPT finds, for the same uncertainty budget, a worse voltage value, i.e. 0.141 p.u.. This means that in case B, due to the presence of ECs, the solver is trapped into a local optimum, since a lower value of the objective is calculated in case B1. Tables V and VI show, for experiment B1, the node voltages and generators reactive power production, respectively. One can observe that several generators reached their limit.

E. Validation on a Real-World System

The findings exposed so far and scalability are tested using a real-world 1203-bus planning model of an European country. This system contains 1203 buses, 177 generators, and more than 500 TSO-DSO interfaces.

TABLE II
FIRST SET OF EXPERIMENTS: WORST-VOLTAGE

	experiment instances					
bus	A	B	C	D	E	F
1011	0.962	0.934	0.923	0.903	0.900	0.985
1012	1.014	0.995	0.988	0.975	0.973	1.028
1013	1.020	1.010	1.006	0.999	0.997	1.031
1022	1.007	0.960	0.940	0.896	0.887	1.060
1041	**0.947**	**0.889**	**0.869**	**0.833**	**0.823**	**0.131**
1042	1.017	1.001	0.996	0.987	0.984	0.993
1043	0.971	0.923	0.906	0.876	0.866	0.455
1044	0.980	0.929	0.912	0.880	0.872	0.882
1045	0.989	0.943	0.928	0.900	0.893	0.834
2031	0.984	0.935	0.917	0.881	0.874	1.030
2032	0.990	0.976	0.971	0.961	0.959	1.007
4071	0.990	0.959	0.947	0.928	0.925	0.988
4072	1.001	0.991	0.988	0.982	0.981	1.005
4041	1.006	0.953	0.934	0.898	0.891	1.050
4042	0.995	0.951	0.936	0.907	0.901	0.999
4043	0.976	0.933	0.918	0.891	0.885	0.965
4046	0.968	0.930	0.917	0.893	0.887	0.968
4047	0.994	0.969	0.961	0.945	0.941	0.993
4051	1.016	0.999	0.993	0.983	0.981	0.990
4061	0.959	0.920	0.907	0.883	0.878	1.018
4062	0.991	0.971	0.964	0.952	0.950	1.015
4063	0.991	0.980	0.976	0.971	0.969	1.014
4012	0.999	0.971	0.961	0.941	0.938	1.017
1014	1.039	1.031	1.028	1.023	1.022	1.046
1021	1.057	1.047	1.043	1.034	1.032	1.068
4011	0.987	0.955	0.943	0.920	0.916	1.010
4021	1.009	0.954	0.933	0.893	0.885	1.053
4022	0.995	0.937	0.914	0.867	0.858	1.057
4032	1.000	0.942	0.920	0.878	0.870	1.037
404c	0.969	0.966	0.966	0.965	0.964	0.880
4031	0.993	0.935	0.914	0.872	0.863	1.045
404f	1.025	1.011	1.007	0.998	0.996	0.976
404g	1.025	1.011	1.007	0.998	0.996	0.976
404d	0.984	0.964	0.957	0.944	0.941	0.933
404e	0.973	0.950	0.942	0.928	0.924	0.829
4044	0.987	0.938	0.921	0.889	0.882	0.934
4045	0.997	0.954	0.939	0.912	0.906	0.894
g1	1.070	1.070	1.070	1.070	1.070	1.070
g2	1.055	1.055	1.055	1.055	1.055	1.055
g3	1.060	1.060	1.060	1.060	1.060	1.060
g4	1.070	1.070	1.070	1.070	1.070	1.070
g5	1.070	1.070	**1.061**	**1.021**	**1.014**	1.070
g6	1.063	1.063	1.063	1.063	**1.062**	1.063
g7	1.054	1.054	1.054	**1.051**	**1.043**	**0.690**
g8	1.004	1.004	1.004	1.004	1.004	1.004
g9	0.999	0.999	0.999	0.999	0.999	0.999
g10	1.002	1.002	1.002	1.002	1.002	1.002
g11	1.034	1.034	1.034	1.034	1.034	1.034
g12	1.014	1.014	1.014	1.014	1.014	1.014
g13	1.000	1.000	1.000	1.000	1.000	1.000
g14	1.011	1.011	1.011	1.011	1.011	1.011
g15	1.061	1.061	1.061	1.061	1.061	1.061
g16	1.061	1.061	1.061	1.061	1.061	1.061
g17	1.045	1.045	1.045	1.045	1.045	1.045
g17b	1.037	1.037	1.037	1.037	1.037	1.037
g18	1.012	1.012	1.012	1.012	1.012	1.012
g19	1.029	1.029	1.029	1.029	1.029	1.029
g20	1.029	1.029	1.029	1.029	1.029	1.029
g21	1.030	1.030	1.030	1.030	1.030	1.030
g22	1.019	1.019	1.019	1.019	1.019	1.019

As the results obtained confirm the findings highlighted for the Nordic system, only the results of the first set of experiments (i.e. with relaxed low voltage) are provided. Fig. 4

TABLE III
FIRST SET OF EXPERIMENTS: GENERATORS REACTIVE POWER AT THE OPTIMAL SOLUTION

	experiment instances					
gen	A	B	C	D	E	F
g1	332.225	438.095	477.556	551.973	565.399	250.153
g2	155.041	199.583	215.958	246.635	252.171	110.973
g3	117.155	154.883	168.859	195.137	199.880	83.989
g4	66.740	107.638	124.845	163.700	171.216	19.943
g5	122.752	206.668	**225.000**	**225.000**	**225.000**	26.528
g6	149.228	193.520	208.211	234.863	**240.000**	217.478
g7	129.162	197.950	221.117	**260.000**	**260.000**	**260.000**
g8	101.809	182.582	212.501	271.312	283.065	8.580
g9	93.740	309.581	390.161	542.518	570.237	-60.834
g10	29.921	178.938	234.770	340.378	359.474	-67.642
g11	64.203	179.213	222.040	305.429	322.011	-26.985
g12	69.367	205.973	257.088	358.184	378.475	-55.620
g13	-18.126	140.840	197.467	304.999	327.031	-149.459
g14	89.983	295.910	368.221	504.214	532.902	68.799
g15	544.772	658.757	698.028	771.082	786.906	551.481
g16	293.593	400.594	437.372	505.660	520.429	299.902
g17	151.096	233.684	260.993	310.350	321.430	278.295
g17b	114.400	196.409	223.526	272.537	283.540	240.707
g18	92.997	175.799	203.112	251.839	261.716	-3.010
g19	167.929	213.176	227.426	251.946	256.753	73.840
g20	167.929	213.176	227.426	251.946	256.753	73.840
g21	146.770	253.825	292.983	360.448	371.433	154.565
g22	706.029	1083.095	1208.322	1406.989	1436.735	403.328

TABLE IV
EXPERIMENTS AND UNCERTAINTY BUDGET

experiment	ρ (%)	$V_i^{\min}$ (p.u.)	worst voltage (p.u.)
C1	27	0.90	0.90
C2	26	0.85	0.869
F1	27	0.80	0.80
F2	27	0.75	0.75
F3	27	0.70	0.70

displays the lowest voltage magnitude obtained at the critical selected bus as uncertainty budget grows. As expected, the larger the uncertainty budget the lower the voltage value.

A loadability limit of the system corresponds to 20.9547% of homothetic load increase. Conversely to the Nordic system, a huge and sharp drop in the worst voltage (0.62 p.u.) occurs a bit before that loadability limit, i.e. at 20% of power uncertainty. Also conversely to the Nordic system, a large number of generators reach their reactive power limit, see Table VIII. The results confirm empirically that all ECs are met as, at the optimum, since all generators maintain their voltage setpoint unless they are at the reactive power limit, in which case their voltage drops.

The computation time of AC OPF with ECs ranges between 4 and 30 seconds, hence it can be used in practice.

IV. DISCUSSION AND CONCLUSION

This paper has proposed and scrutinized the new problem of calculating the worst-voltage-case under power flows uncertainty, particularly at TSO-DSO interfaces. Such calculation is important as it supports a TSO in identifying potentially dangerous situations where the uncertainty in distribution grids operation endangers transmission grid voltage stability.

TABLE V
SECOND AND THIRD SETS OF EXPERIMENTS: WORST-VOLTAGE

	experiment instances				
bus	F1	F2	F3	C1	B1
1011	0.889	0.889	0.898	0.962	0.873
1012	0.966	0.967	0.974	1.015	0.944
1013	0.993	0.994	0.998	1.022	0.989
1022	0.861	0.849	0.837	0.995	0.679
1041	**0.800**	**0.750**	**0.700**	**0.900**	**0.141**
1042	0.963	0.931	0.896	1.005	0.985
1043	0.842	0.797	0.747	0.933	0.444
1044	0.850	0.816	0.770	0.942	0.851
1045	0.874	0.844	0.808	0.954	0.813
2031	0.851	0.834	0.803	0.954	0.949
2032	0.952	0.948	0.940	0.984	0.984
4071	0.916	0.931	0.959	1.003	0.419
4072	0.979	0.994	1.002	1.013	0.210
4041	0.868	0.846	0.810	0.970	0.998
4042	0.883	0.853	0.807	0.965	0.964
4043	0.867	0.838	0.794	0.944	0.934
4046	0.872	0.845	0.804	0.940	0.941
4047	0.931	0.910	0.877	0.976	0.975
4051	0.974	0.965	0.961	1.003	0.981
4061	0.863	0.852	0.839	0.935	0.991
4062	0.943	0.939	0.935	0.984	1.003
4063	0.966	0.971	0.972	0.996	1.008
4012	0.927	0.928	0.936	0.999	0.890
1014	1.019	1.020	1.023	1.040	1.013
1021	1.027	1.024	1.022	1.054	0.989
4011	0.903	0.903	0.911	0.985	0.880
4021	0.860	0.842	0.814	0.982	0.991
4022	0.830	0.817	0.804	0.977	0.820
4032	0.843	0.819	0.777	0.965	0.962
404c	0.962	0.938	0.903	0.960	0.878
4031	0.836	0.816	0.778	0.960	0.949
404f	0.990	0.980	0.971	1.017	0.980
404g	0.990	0.980	0.971	1.017	0.980
404d	0.933	0.904	0.865	0.970	0.934
404e	0.913	0.886	0.856	0.955	0.829
4044	0.861	0.830	0.786	0.951	0.901
4045	0.888	0.861	0.827	0.965	0.871
g1	1.070	1.070	1.070	1.070	1.069
g2	1.055	1.055	1.055	1.055	1.055
g3	1.060	1.060	1.060	1.060	1.060
g4	1.070	1.070	1.070	1.070	1.070
g5	**0.989**	**0.979**	**0.968**	1.070	**0.213**
g6	**1.042**	**1.013**	**0.980**	1.063	1.063
g7	**1.022**	**0.983**	**0.939**	1.054	**0.680**
g8	1.004	1.004	1.004	1.004	1.004
g9	0.999	0.999	0.999	0.999	0.999
g10	1.002	1.002	1.002	1.002	1.002
g11	1.034	1.034	1.034	1.034	1.034
g12	1.014	1.014	**0.991**	1.014	1.014
g13	1.000	1.000	1.000	1.000	1.000
g14	1.011	**0.987**	**0.946**	1.011	1.011
g15	1.061	1.061	1.061	1.061	1.061
g16	1.061	**1.046**	**1.016**	1.061	1.061
g17	1.045	1.045	1.045	1.045	1.045
g17b	1.037	1.037	1.037	1.037	1.037
g18	1.012	1.012	1.012	1.012	1.012
g19	1.029	1.029	1.029	1.029	1.029
g20	1.029	1.029	1.029	1.029	1.029
g21	1.030	1.030	1.030	1.030	**0.645**
g22	1.019	1.019	1.019	1.019	**0.447**

Such situation needs planning mitigation actions in the case harmful uncertainty materializes. Also, solving rigorously such problem is vital for developing successful robust (i.e. worst-case-based) optimization approaches to AC SCOPF.

TABLE VI
SECOND AND THIRD SETS OF EXPERIMENTS: GENERATORS REACTIVE POWER AT THE OPTIMAL SOLUTION

	experiment instances				
gen	F1	F2	F3	C1	B1
g1	605.973	601.467	561.263	323.016	**720.000**
g2	268.640	266.081	247.942	146.170	287.489
g3	214.103	212.290	197.513	111.894	244.269
g4	194.910	205.225	215.954	76.663	356.944
g5	**225.000**	**225.000**	**225.000**	143.128	**225.000**
g6	**240.000**	**240.000**	**240.000**	181.655	**240.000**
g7	**260.000**	**260.000**	**260.000**	183.658	**260.000**
g8	319.813	345.578	388.503	137.774	140.689
g9	654.646	653.253	598.448	108.964	809.877
g10	417.379	412.941	365.817	32.903	613.428
g11	374.244	412.733	469.823	121.058	102.286
g12	442.295	492.049	**515.000**	147.165	172.614
g13	394.954	462.118	569.996	90.772	6.425
g14	620.336	**630.000**	**630.000**	232.633	236.358
g15	834.636	930.622	1081.50	628.835	632.377
g16	564.929	**580.000**	**580.000**	372.542	375.864
g17	353.348	399.113	420.717	214.811	320.125
g17b	315.235	360.680	382.134	177.668	282.244
g18	290.998	303.924	322.430	124.477	46.166
g19	270.788	250.827	247.027	145.923	99.054
g20	270.788	250.827	247.027	145.923	99.054
g21	401.858	350.029	254.524	102.054	**520.000**
g22	1512.850	969.556	636.927	244.934	**4000.00**

TABLE VII
EXPERIMENTS AND UNCERTAINTY BUDGET

experiment	ρ (%)	V_i^{initial} (p.u.)	worst voltage (p.u.)
B1	25	< 0.75	0.141
B2	25	> 0.80	0.889

This paper has proposed a tailored AC OPF formulation to calculate the worst voltage, which most notably models by ECs the generator switch from under voltage control to under reactive power limit. This switch allows generator' voltage to drop and thereby explore the lower part of the PV curve.

The paper has conducted a series of experiments on the 60-bus Nordic system and a real 1203-bus grid that have

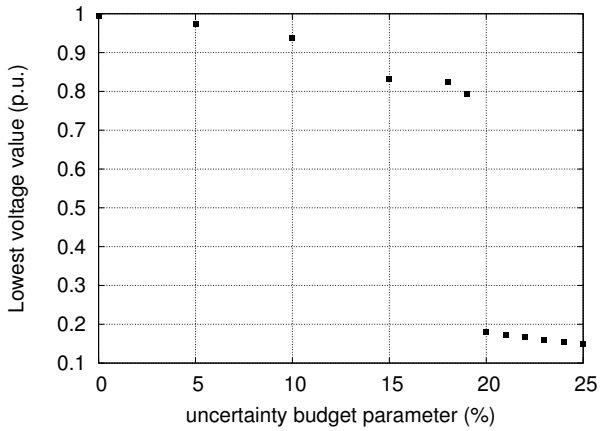

Fig. 4. Worst voltage versus uncertainty budget.

TABLE VIII
UNCERTAINTY BUDGET

ρ (%)	worst voltage (p.u.)	number of generators losing voltage control
0	0.994	0
5	0.973	1
10	0.938	16
15	0.831	20
18	0.825	23
19	0.794	25
20	**0.179**	28
21	**0.172**	29
22	**0.166**	31
23	**0.159**	32
24	**0.154**	34
25	**0.148**	36

pointed out the challenges associated to such computations and revealed new insights. The results show that, on the one hand, when the low voltage limit is relaxed, the voltage initialization can affect the mathematical solution obtained due to the presence of local optima that correspond to different sets of binding generators' reactive power limits. In the absence of a system dynamic model, one cannot rule out whether mathematically low voltage solutions (e.g. around 0.1 p.u.) may not be also physical solutions that can be reached by the realization of the worst uncertainty. Further research is needed to evaluate if the lowest voltage solutions calculated are physically meaningful. On the other hand, if one imposes a lower voltage bound, it may impact the worst-voltage calculation, conditioning its result and hiding the true worst value. For instance, if the uncertainty budget can lead to infeasible problems, the uncertainty is adjusted such that the low voltage limit is always reached, stopping the degradation to the worst possible voltage corresponding to this uncertainty budget.

It was empirically demonstrated that, for a given budget of uncertainty, lowering the voltage limit allows fully exploring the lower part of the PV curve widely used in voltage stability analysis. However, searching the lowest voltage magnitude at a node and imposing a lower limit on it in the optimization problem are conflicting. Indeed, imposing a low voltage limit prevents computing the true worst-case as the uncertainty is not allowed to lead to infeasible cases. The only practical solution to circumvent these issues is to impose a realistic low voltage limit; this aspect requires further research.

Finally, this distinct work overlaps to some extent to other researches that calculate: static loadability margins and limits with respect to voltage stability [20], low voltage power flow solutions (exploring the lower part of a PV curve) [23], [22], [24], and local optima in AC OPF [25].

Future work will enhance the model with additional ECs expressing the generator trip by protection at low voltages and adapt the proposed approach to AC SCOPF problems [26].

REFERENCES

[1] M. Rossi, G., Migliavacca, G., Vigano et al., "TSO-DSO coordination to acquire services from distribution grids: Simulations, cost-benefit analysis and regulatory conclusions from the SmartNet project", *Electric Power Systems Research*, 189, 106700, 2020.

[2] M. Usman, M.I. Alizadeh, F. Capitanescu, I. Avramidis, A.G. Madureira "A novel two-stage TSO-DSO coordination approach for managing congestion and voltages", *International Journal of Electrical Power & Energy Systems* 147, 108887, 2022.

[3] G. Valverde, D. Shchetinin, G. Hug-Glanzmann, "Coordination of distributed reactive power sources for voltage support of transmission networks", *IEEE Trans. Sust. Energy*, vol. 10, no. 3, pp. 1544-1553, 2019.

[4] L.D.P Ospina, T. Van Cutsem, "Emergency support of transmission voltages by active distribution networks: A non-intrusive scheme" *IEEE Trans. Pow. Syst.*, vol. 36, no. 5, pp. 3887-3896, 2020.

[5] F. Escobar, J.M. Viquez, J. Garcia, P. Aristidou, G. Valverde, "Coordination of DERs and Flexible Loads to Support Transmission Voltages in Emergency Conditions", *IEEE Trans. Sust. Energy*, vol. 13, no. 3, pp. 1344-1355, 2022.

[6] F. Capitanescu, Challenges ahead risk-based AC optimal power flow under uncertainty for smart sustainable power systems, Invited chapter in the book "Dynamic Vulnerability Assessment and Intelligent Control for Sustainable Power Systems" (Eds: F. Gonzalez Longatt and J.L. Rueda Torres). John Wiley & Sons, Inc, 2018.

[7] J. Jarjis, F.D. Galiana, "Quantitative analysis of steady state stability in power networks", *IEEE Trans. on Power Apparatus and Systems*, vol. PAS-100, no. 1, 1981, pp. 318-326.

[8] D. Gan, X. Luo, D.V. Bourcier, R.J. Thomas, "Min-Max Transfer Capability of Transmission Interfaces", *International Journal of Electrical Power and Energy Systems*, vol. 25, no. 5, 2003, pp. 347-353.

[9] I. Dobson, L. Lu, "New methods for computing a closest saddle node bifurcation and worst case load power margin for voltage collapse", *IEEE Trans. on Power Systems*, vol. 8, no. 2, 1993, pp. 905-911.

[10] F. Capitanescu, T. Van Cutsem, "Evaluating bounds on voltage and thermal security margins under power transfer uncertainty", *Proc. of the PSCC Conference*, Seville (Spain), June 2002.

[11] A. Lorca, X.A. Sun, "The adaptive robust multi-period alternating current optimal power flow problem", *IEEE Trans. on Power Systems*, vol. 33, no. 2, pp. 1993-2003, 2017.

[12] R. Louca, E. Bitar, "Robust AC optimal power flow", *IEEE Trans. on Power Systems*, vol. 34, no. 3, pp. 1669-1681, 2018.

[13] D. Lee, K. Turitsyn, D.K. Molzahn, L. Roald, "Robust AC Optimal Power Flow with Convex Restriction", *IEEE Trans. on Power Systems*, vol. 36, no. 6, pp. 4953-4966, 2021.

[14] F. Capitanescu, S. Fliscounakis, P. Panciatici, L. Wehenkel, "Cautious operation planning under uncertainties", *IEEE Trans. on Power Systems*, vol. 27, no. 4, pp. 1859-1869, 2012.

[15] F. Capitanescu, L. Wehenkel, "Computation of worst operation scenarios under uncertainty for static security management", *IEEE Trans. on Power Systems*, vol. 28, no. 2, pp. 1697-1705, 2013.

[16] N. Yorino, M. Abdillah, Y. Sasaki, Y. Zoka, "Robust power system security assessment under uncertainties using bi-level optimization", *IEEE Trans. on Power Systems*, vol. 33, no. 1, pp. 352-362, 2017.

[17] F. Capitanescu, W. Rosehart, L. Wehenkel, "Optimal power flow computations with constraints limiting the number of control actions", IEEE PowerTech conference, Bucharest (Romania), 2009.

[18] PGLib-opf-case60, https://github.com/power-grid-lib/pglib-opf

[19] GAMS platform version 28.2, 2019. Available online: www.gams.com.

[20] S.G. Ghiocel, J.H. Chow, "A power flow method using a new bus type for computing steady-state voltage stability margins", *IEEE Trans. on Power Syst.* vol. 29, no. 2, pp. 958-965, 2013.

[21] A. Wachter, L.T. Biegler, "On the implementation of an interior-point filter line-search algorithm for large-scale nonlinear programming", Mathematical programming vol. 106, no. 1, 2006, pp. 25-57.

[22] T.J. Overbye, R.P. Klump, "Effective calculation of power system low-voltage solutions", *IEEE Trans. Pow. Syst.*, vol. 11, no. 1, pp. 75-82, 1996.

[23] W. Ma, S. Thorp, "An Efficient Algorithm to Locate All the Load Flow Solutions", *IEEE Trans. Pow. Syst.*, vol. 8, no. 3, pp. 1077-1083, 1993.

[24] D.K. Molzahn, B.C. Lesieutre, H. Chen, "Counterexample to a continuation-based algorithm for finding all power flow solutions", *IEEE Trans. on Power Syst.* vol. 28, no. 1, pp. 564-56, 2012.

[25] D. Wu, D.K. Molzahn, B.C. Lesieutre, K. Dvijotham, "A deterministic method to identify multiple local extrema for the ac optimal power flow problem", *IEEE Trans. on Power Syst.*, vol. 33, no. 1, pp. 654-668, 2017.

[26] F. Capitanescu, M. Glavic, D. Ernst, L. Wehenkel, "Applications of security-constrained optimal power flows", in Proceedings of Modern Electric Power Systems Symposium (MEPS), Wroclaw (Poland), 2006.